Fundamentals of Metal Deposition via Surface Limited Redox Replacement of Underpotentially-Deposited Monolayer

by Stanko R. Brankovic

Deposition via surface limited redox replacement (SLRR) of underpotentially-deposited (UPD) monolayer (ML)[1] has gained many applications in the last two decades.[2-4] The caveat of this deposition method is the use of the M UPD ML as sacrificial material to reduce/deposit a more noble metal P (galvanic displacement). Over the years, several experimental protocols have been developed. The first basic protocol[1,5] involves formation of a UPD ML of M on the substrate S(h,k,l) (potential controlled step) and then subsequent immersion of M_{UPD}/S(h,k,l) in a separate solution where SLRR occurs and deposition of P takes place at open circuit (sample shuffling approach). The second protocol involves a similar routine but with a stagnant substrate; the solutions for M UPD ML formation and P deposition are exchanged in a single SLRR cycle[6] (solution shuffling approach). Finally, the latest developed protocol adopts a *one-solution, one-cell* experimental design.[7,8] In this case, the same solution serves for UPD ML formation and subsequent SLRR reaction at opencircuit potential. In a first potential-controlled step, co-deposition of UPD ML of M with small amount of P occurs, then the potential control is turned off (opencircuit step), allowing the SLRR reaction and deposition of P to proceed. The details of these three protocols have been frequently discussed in literature[4,5,9] and examples are presented also in this issue of *Interface*.

In many applications concerned with deposition of only a single monolayer of P or ultra-thin films such as core-shell catalyst synthesis for example[2,3,5] (P = Pt, Ru, Pd), the properties of deposited films are a direct function of their morphology.[10-15] Although the basic role of the UPD ML serving as a reducing agent for noble metal ions can be understood from fundamental electrochemical perception, successful control of the deposit morphology requires deeper insight. Specifically, the SLRR reaction stoichiometry, thermodynamics and kinetics and how these relate to the nucleation process[11,16] on the one hand and the experimental conditions[5,17] on the other. Therefore, identifying and understanding the fundamental relation between the experimental conditions and processes involved in deposition via SLRR reaction is mandatory if one is to claim full control over the deposit morphology. The aim of this article is to convey these relations using commonly adopted terminology and to point to some opportunities for future developments of this method.

Underpotential Deposition—The First Step and Enabling Phenomenon

Many electrochemical systems that include a noble metal electrode in solution with different metal ions exhibit the UPD phenomenon. It is diagnosed by the formation of one or two *wetting* monolayers (MLs) on the electrode surface at potentials that are more positive than the equilibrium potential defined by Nernst equation. In the 1960s and 1970s, extensive studies of many UPD systems were performed on single crystal and polycrystalline electrodes.[18,19] With the development of different in situ surface characterization methods during the 1980s and 1990s, many UPD systems were re-examined in detail, unraveling more information about the UPD process, its mechanisms and diversity.[20,21]

UPD represents a potential dependent adsorption with great sensitivity and selectivity towards the nature of the metal surface and its termination. The characteristic cyclic voltammetry features associated with the UPD process are demonstrated by one or more deposition/stripping peaks in the underpotential region observed during the potential sweep in the cathodic/anodic direction. The complexity of the voltammetry features arises from the existence of one or more UPD ML superstructures[22,23] and/or one or more UPD MLs formed.[24,25] An example of UPD cyclic voltammograms (CVs) is shown in Fig. 1 for two UPD systems commonly used in deposition via SLRR of UPD ML.

Over the years, different analytical models were developed to explain the UPD as a potential dependent adsorption process.[26-29] The adsorption behavior, in the most cases, is determined by the attractive interactions between the UPD metal and the substrate, and the repulsive interactions between the adatoms within the UPD ML. However, the effect of stored elastic energy in the UPD ML due to the epitaxial strain and the energetics of the anion co-adsorption were found to be important as well. In the quest for proper description of the UPD system one usually resorts to the analytical expression which best describes the underpotential vs. coverage relation, i.e., the UPD isotherm. The Burkenstain-Shwatterian (BS) isotherm is the most general one and offers sufficient depth for the interpretation for most UPD systems. It is formulated as follows:[30]

$$\Delta E = \Delta E^{0}_{\theta\to 0} - \frac{RT}{m\cdot F}\cdot\left[\ln\left(\frac{\theta}{1-\theta}\right) + f\theta + g\theta^{3/2}\right] \quad (1)$$

Here the $\Delta E^{0}_{\theta\to 0}$ term represents the underpotential of the most positive stripping peak of the UPD adlayer where its coverage approaches zero. The term f is the Temkin parameter describing the attractive UPD ML-substrate interactions. The term g is the Frumkin parameter representing the lateral adatom interactions within the UPD ML. Examples of fits of the BS isotherm to θ vs. ΔE data for the two UPD systems in Fig. 1A are shown in Fig. 1B.

Stoichiometry of the Surface Limited Redox Replacement Reaction

The UPD ML coverage can be controlled effectively down to a fraction of a monolayer by proper choice of an underpotential (Fig. 1B). Accordingly, the same accuracy, for the coverage of metal P deposited via SLRR of the UPD M ML is expected. The amount/coverage of deposited P is controlled by the reaction stoichiometry, and the structure and coverage of the UPD ML of metal M. The most general formulation of the SLRR reaction is given by the following equation:[16]

$$\left(\theta_M\cdot\rho_M^{UPD}\right)\cdot M^{0}_{UPD}/S(h,k,l) + \left(\theta_M\cdot\rho_M^{UPD}\right)\cdot\left(\frac{m}{p}\right)P^{p+}_{solv} \Rightarrow \left(\theta_M\cdot\rho_M^{UPD}\right)\cdot M^{m+}_{solv} + \left(\theta_M\cdot\rho_M^{UPD}\right)\cdot\left(\frac{m}{p}\right)P^{0}_{s}/S(h,k,l) \quad (2)$$

Here, m and p are the oxidation states of the UPD metal M and the more noble metal P. They are also the stoichiometry coefficients in the SLRR equation. Factors θ_M, and ρ_M^{UPD} are, respectively, the UPD

(continued on next page)

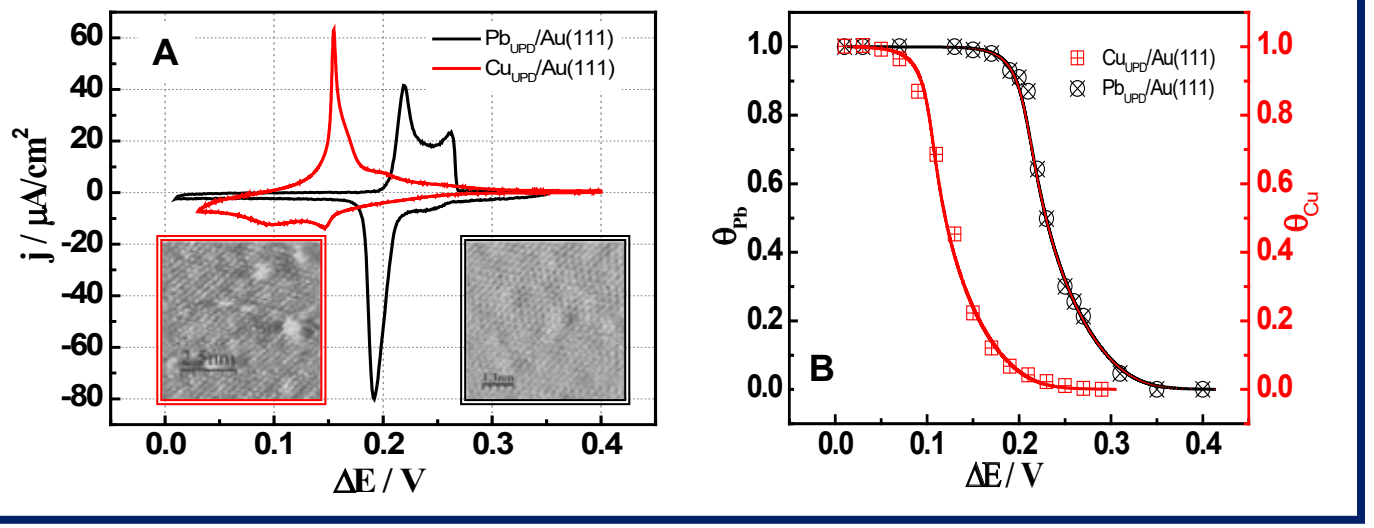

Fig. 1. *(A) Cyclic voltammograms for Pb UPD on Au(111) (black) and Cu UPD on Au(111) (red). Solution: 10^{-3} M Pb^{2+} (Cu^{2+}) + 0.1 M $HClO_4$, sweep rate 10 mV·s^{-1}. Insets show atomic resolution of full Cu UPD layer (red) and full Pb UPD layer (black) on Au(111). (B) Coverage θ versus ΔE dependence for Cu UPD on Au(111), (red) and Pb UPD on Au(111), (black). The coverage is estimated from charge stripping experiments. The full lines represent fits of the BS isotherm model to the coverage data (see text for more details).*

ML coverage and the packing density of M atoms in the full UPD ML with respect to the underlying substrate S(h,k,l). These parameters serve to accurately express the amount of deposited metal P in ML units with respect to the substrate S(h,k,l). In many reports, they are commonly omitted as the authors use consolidated SLRR equation defined only in terms of the stoichiometry coefficients. These presentations generally lack the full information about the expected deposit coverage in a single SLRR cycle. For example, if the metal P forms a 2D-monoatomically thick deposit, one can easily deduce, from Eq. 2, the expected P coverage with respect to the atomic areal density of the substrate. It is defined as:[16]

$$\theta_P = \theta_M \cdot \rho_M^{UPD}\left(\frac{m}{p}\right) \qquad (3)$$

Practitioners should be aware that the overall stoichiometry of the SLRR reaction also depends on specific experimental conditions favoring one over the other oxidation states of the metal M constituting the UPD ML. A typical example is copper which is stable either as the Cu^+ or Cu^{2+} ion. Direct ligand transfer from depositing noble metal ion complexed with halides ($\{PX_n\}^{(p-n)}$, P = Pt, Pd, Ru, X = Cl^-, Br^-…) to dissolving Cu ions could stabilize a $\{CuX_2\}^-$ complex where Cu has the +1 oxidation state.[16] This situation is generally applicable to experiments where the supporting electrolyte in the SLRR solution does not contain anions with complexing/stabilizing ability towards Cu^{2+} such as $\{ClO_4\}^-$ for example. Therefore, one should make sure to know the main complexing ligands at the interface when considering the stoichiometry of the SLRR of Cu UPD ML.

Driving Force for the SLRR Reaction and Nucleation Rate of Depositing Metal

The electrochemical driving force for SLRR reaction between the P^{p+} and M UPD ML is the positive difference between equilibrium potential of the bulk P and equilibrium potential of the M UPD ML at its coverage approaching zero limit, $\theta_{UPD} \rightarrow 0$.[1] This condition is defined as:

$$\Delta E_{SLRR} = \Delta E^0_{EMF} - \Delta E^0_{\theta\to 0} - \frac{RT}{F}\ln\frac{\left[a_{M^{m+}}\right]^m}{\left[a_{P^{p+}}\right]^p} > 0 \qquad (4)$$

Here, ΔE^0_{EMF} $\left(\Delta E^0_{EMF} = E^0_{P^{p+}/P} - E^0_{M^{m+}/M}\right)$ represents the electromotive force for the bulk M and P galvanic couple at standard conditions. The $\Delta E^0_{\theta\to 0}$ is the equilibrium underpotential of M UPD ML at the $\theta_{UPD} \rightarrow 0$ limit (UPD shift) at standard conditions ($a_{M^{m+}} = 1$, $a_{P^{p+}} = 1$, where *a* stand for activity). The logarithmic term provides a correction for the departure from standard conditions. In general, for most systems involving a noble metal ion-UPD metal ML, the condition described by Eq. 4 is always satisfied (Ag and Pd UPD MLs might be the only exceptions). It is important to recognize that ΔE_{SLRR} can be modified by adjusting the activities of M^{m+} and P^{p+} ions in the reaction solution, Eq. 4. Assuming that the ion concentrations are a good approximation for the activity of metal ions, it is a straightforward exercise to show that the nucleation overpotential and nucleation rate (J ~ exp(−*const*/$(\Delta E_{SLRR})^2$))[31]are effectively controlled by the metal ions concentration. Clearly, the link between the experimental

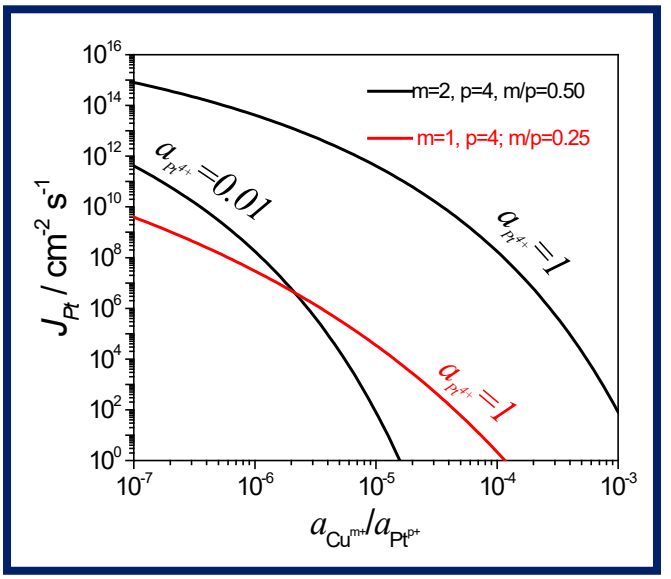

Fig. 2. *Estimates of the Pt nucleation rate versus $a_{Cu^{m+}}$ / $a_{Pt^{4+}}$ ratio. Estimates are made for Pt deposition via SLRR of Cu UPD ML. SLRR reactions:*
$2Cu^0_{UPD} + \{PtCl_6\}^{2-} = Pt^0 + 2Cu^{2+} + 6Cl^-$ (black).
$4Cu^0_{UPD} + \{PtCl_6\}^{2-} + 2Cl^- = 4\{CuCl_2\}^- + Pt^0$ (red).

conditions and nucleation behavior of the system is rooted in the dependence of ΔE_{SLRR} on the SLRR reaction stoichiometry and the metal ion concentrations in the reaction solution.

The special case for ΔE_{SLRR} is when there are no M^{m+} in the reaction solution. Then, the logarithmic term is very large and its contribution dominates the value of ΔE_{SLRR}. This leads to high nucleation rates of P and formation of very small 2D nuclei on the surface. This discussion is qualitatively illustrated in Fig. 2. Using classical nucleation theory,[31] the nucleation rate is approximately calculated for Pt deposition on Au(111) via SLRR of Cu UPD ML. For the two scenarios discussed previously (Cu^{+} vs. Cu^{2+}), the nucleation rate is shown as a function of $a_{Cu^{m+}} / a_{Pt^{4+}}$ ratio. One can see that a change in the experimental conditions leading to a 10× decrease in $a_{Cu^{m+}} / a_{Pt^{4+}}$ produces approximately a 10^3 – 10^5 times higher nucleation rate. A similar effect is achieved by 100× dilution of Pt^{4+} while keeping the same $a_{Cu^{m+}} / a_{Pt^{4+}}$ ratio. It has to be mentioned that the calculations in Fig. 2 are considered only as an illustration of the qualitative trend in nucleation rate induced by the changes in reaction stoichiometry (m/p ratio) and solution design ($a_{Cu^{m+}} / a_{Pt^{4+}}$). The conclusion that one takes from this discussion is that the SLRR reactions with larger m/p ratio and solutions with smaller $a_{M^{m+}} / a_{P^{p+}}$ ratio yield higher nucleation rates and thus a P deposits consisting of smaller clusters.

Reaction Kinetics vs. Nucleation Kinetics

Thermodynamics arguments formulate a correct framework for understanding the trends in deposit morphology dependence on experimental conditions of SLRR. Nevertheless, they are insufficient to elucidate all mechanistic details of the nucleation process. For this reason, other approaches were developed to establish a complete understanding of the phenomena controlling the deposition via SLRR of UPD ML. Following theoretical considerations from nucleation kinetics,[32,33] generalized results from recent work show that the nucleation density of P obtained during SLRR of UPD ML of metal M is well described by the following relation:[11]

$$n_P^{SLRR} = \alpha_0 \left(1 - \chi \cdot \theta_{o,M}\right) \cdot \left(\theta_{o,M}\right)^{N/3} \quad (5)$$

Here, n_P^{SLRR} is given in cm^{-2} units and α_0 is the numerical constant defined as $\alpha_0 = \left[\frac{m}{p} \cdot \frac{\Gamma_M^{UPD} K_{SLRR}}{D_P^S \cdot a^2}\right]^{1/3}$. K_{SLRR} is the SLRR reaction rate constant in s^{-1} units, Γ_M^{UPD} is the surface concentration of the full UPD ML in $mol \cdot cm^{-2}$ units, D_P^S is the surface diffusivity of P adatoms over the substrate S(h,k,l) in $cm^2 \cdot s^{-1}$ and a is the nearest neighbor distance on the surface (cm). The term χ is the numerical constant defined as $1-(n_P)$ where (n_P) stands for the nucleation probability of P on top of the M UPD ML.[11] $\theta_{o,M}$ represents the initial coverage of the UPD ML and the N is the SLRR reaction order in terms of the UPD ML as reactant. Equation 5 only applies for reaction orders where N > 0, i.e., for true SLRR reaction kinetics. When N > 1, the rate constant is defined as follows:[17]

$$K_{SLRR} = (N-1) \cdot k \cdot \left(C_P^{is}\right)^L \cdot \left(\Gamma_M^{UPD}\right)^{N-1} \quad (6)$$

Here, k represents the fundamental rate constant, C_P^{is} is the concentration of P^{p+} at the interface in $mol \cdot cm^{-2}$ units and L is the SLRR reaction order in terms of P^{p+} as reactant. For any practical consideration, C_P^{is} can be expressed as the product of the bulk concentration C_P^{∞}, $(mol \cdot dm^{-3})$ and the interface width $\xi \left(\approx 10^{-7} \text{ cm}, C_P^{is} = C_P^{\infty} \cdot \xi\right)$. For the case N = 1, the rate constant is defined as follows:[17]

$$K_{SLRR} = k\left(C_P^{is}\right)^L \quad (7)$$

The proper determination of the reaction order and rate constant during SLRR of UPD ML is a somewhat challenging task.[17,34]

To a first approximation, the value of N can be taken from the SLRR reaction stoichiometry assuming that it is an elementary red-ox process. However, a more proper methodology for the determination of the SLRR reaction kinetics parameters requires in situ measurements that monitor the UPD ML coverage during the reaction. One way to do this is by measuring the surface reflectivity during SLRR reaction and fitting the obtained data by an appropriate rate equation to extract the rate constant and reaction order.[34] Another way to do this is by measuring the open circuit potential (OCP) during the SLRR reaction.[17] This approach is somewhat easier to implement. It requires the derivation of an analytical model for the dependence of E vs. t during the SLRR reaction to fit the experimental OCP data and extract the parameters of the reaction kinetics.[17] The E versus t models are obtained by combining the appropriate rate equation[35] with a representative UPD adsorption isotherm, such as Eq. 1. Results from such an analysis are shown in Table I below.[36]

Equation 5 represents a bell-shape function whose maximum (n_P^{SLRR} = max) occurs for $\theta_{o,M} = N/(\chi(3+N)$, Fig. 3. n_P^{SLRR} is proportional to α_0. Hence, with proper choice of $\theta_{o,M}$ as well as by careful design of the SLRR reaction and experimental conditions governing α_0, it is possible to control n_P^{SLRR} and achieve the desired average cluster size of the P deposit $\left(\bar{S}_P = \theta_P / n_P^{SLRR} = (m/p) \cdot \theta_{o,M} \cdot \rho_M^{UPD} / n_P^{SLRR}\right)$[10,11].This is of particular importance for the catalysis community where finite size effects are shown to dominate the Pt ML catalyst activity.[10,15,37] Control of the nucleation density and the average cluster size in a single SLRR cycle is also of great interest for thin film growth applications. Homo- and hetero-epitaxial systems that exhibit 3D growth at room temperature due to kinetics limitation can be effectively forced to grow in 2D mode by enhancing the nucleation density and producing smaller nuclei during the growth process.[38]

To illustrate the arguments presented here, we focus on Fig. 3 where plots of Eq. 5 are presented using SLRR kinetics parameters from Table I. The case N = 4 is the starting point in the discussion (bold red). First, we address the effect of K_{SLRR} on n_P^{SLRR}. By definition, K_{SLRR} is proportional to the bulk concentration of P (Pt) ions, Eq. 6 and Eq. 7. A 100× dilution of $\{PtCl_6\}^{2-}$ ions, (from 10^{-3} M to 10^{-5} M $\{PtCl_6\}^{2-}$) results in a 40× decrease in K_{SLRR} (Table I). Considering that $\alpha_0 \sim (K_{SLRR})^{1/3}$, an approximately 3.5× lower nucleation rate is expected. The calculated functional relation between n_{Pt}^{SLRR} and $\theta_{o,Cu}$ for 10^{-5} M $\{PtCl_6\}^{2-}$ is shown in Fig. 3 as a green dashed line. The mathematical form of the relation does not change and evidently, higher concentration of $\{PtCl_6\}^{2-}$ would produce qualitatively the same effect but in the opposite direction, i.e., n_{Pt}^{SLRR} would increase 3.5×.

(continued on next page)

Table I. Parameters for SLRR reaction kinetics extracted from OCP measurements.

SLRR Reaction	Solution, ω = 1000 rpm	K_{SLRR}, $[s^{-1}]$	N	m/p	Ref.
$Cu^0_{UPD} + \frac{m}{p}Pt^{p+}_{solv.} = Cu^{m+}_{solv.} + \frac{m}{p}Pt^0_s$	10^{-3} M $\{PtCl_6\}^{2-}$ + 0.1 M H_2SO_4	4.08 ± 0.07	2[a]	0.5	17
	10^{-3} M $\{PtCl_6\}^{2-}$ + 0.1 M $HClO_4$	3.61 ± 0.03	2[b], 4[a]	0.25	17
	10^{-5} M $\{PtCl_6\}^{2-}$ + 0.1 M $HClO_4$	0.089 ± 0.0008	2[b], 4[a]	0.25	17

[a]Reaction order is taken based on the value of stoichiometry coefficients.
[b]Reaction order determined from the fits of the reaction kinetics model to the open circuit transients obtained during SLRR reaction.

Based on this discussion, one concludes that the nucleation density and nanocluster size is a strong function of the P^{p+} ($\{PtCl_6\}^{2-}$) concentration and the initial coverage of the UPD ML, $\theta_{o,M}$ ($\theta_{o,Cu}$).

The choice of supporting electrolyte in the SLRR reaction involving Cu UPD ML has a decisive effect on the oxidation state of Cu. In the case of 0.1 M $HClO_4$, Table I, the absence of solution complexing ability for Cu^{2+} makes the Cl^- liberated from $\{PtCl_6\}^{2-}$ the only ligand at the interface.[16] This leads to formation of the $\{CuCl_2\}^-$ complex with Cu being +1 oxidation state and m/p = 0.25. However, if the reaction solution has an abundance of sulfate ions, (for example: 0.1 M H_2SO_4) the Cu oxidation state in the SLRR reaction is +2. It means that the m/p ratio is 0.5. The reaction rate constant in this electrolyte is slightly higher too (K_{SLRR} = 4.08 s^{-1}, Table I). Both effects increase the value of α_0 by approximately 30% . The additional outcome is that the reaction order in the case of a 0.1 M H_2SO_4 electrolyte changes to N = 2.[17] This changes the qualitative shape of the n_{Pt}^{SLRR} versus $\theta_{o,Cu}$ curve and the position of the maximum shifts to $\theta_{o,Cu} \approx 0.4$. Therefore, for the same concentration of Pt ions in solution (10^{-3} M) but with a 0.1 M H_2SO_4 supporting electrolyte, roughly 30% higher n_{Pt}^{SLRR} values are expected in the $0 < \theta_{o,Cu} < 1$ range with qualitatively different n_{Pt}^{SLRR} dependence on $\theta_{o,Cu}$, (Fig. 3, blue dashed line). Following the same logic, further enhancement in nucleation density should be expected if the $\{PtCl_6\}^{2-}$ ion is replaced with $\{PtCl_4\}^{2-}$ yielding m/p = 1. In this case, α_0 is approximately 60% larger than the original one. In addition, one Pt ion reacts with one Cu UPD adatom and the reaction order takes N = 1.[17,36] Both changes make a major impact on the n_{Pt}^{SLRR} versus $\theta_{o,Cu}$ dependence even if the K_{SLRR} remains the same (Fig. 3, black line). The maximum value of n_{Pt}^{SLRR} increases almost 75% and further shifts toward the lower values of $\theta_{o,Cu}$ ($\theta_{o,Cu}$ = 0.23, for n_{Pt}^{SLRR} = max). The overall conclusion is that a larger m/p ratio produces a higher nucleation density and a deposit with smaller nanoclusters. The opposite is true when the reaction order is considered. The higher the SLRR reaction order, the lower the nucleation density is, i.e., a deposit with larger nanoclusters is expected.

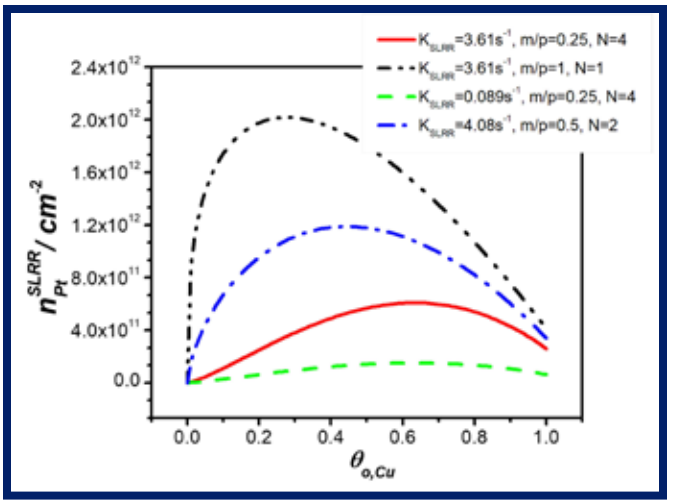

FIG. 3. *Model predictions (Eq. 5) for n_{Pt}^{SLRR} versus $\theta_{o,Cu}$ dependence on SLRR reaction kinetics parameters from Table I. Parameters of the model:*[11] D_{Pt}^{S} / cm^2s^{-1} = 3.5 × 10^{-8}; χ = 0.9; Γ_{Cut}^{UPC} /cm^{-2} = 1.15 × 10^{15}; *a*/cm = 0.408 × 10^{-7}.

An additional way to alter the values of K_{SLRR} and n_P^{SLRR} is by manipulating the experimental conditions that directly influence the fundamental rate constant k. Studies of the SLRR reaction kinetics during Au deposition via SLRR of Pb UPD ML using a *one-solution, one-cell* protocol show that k is linearly dependent on Pb^{2+} concentration, C_{Pb}^{∞}, Fig. 4A.[34] A higher concentration of Pb^{2+} leads to larger values of k. 100% increase in the value of k (or kξ) is observed for one order of magnitude increase in Pb^{2+} concentration. Considering the generalized notation adopted throughout the manuscript, we can state that experimental data in Fig. 4A indicate $k = f(C_M^{\infty})$. The k dependence on C_M^{∞} can be explained by looking into the intrinsic relations between the definitions for the fundamental rate constant,[39] $k \sim \exp(-\Delta G^{\#}/RT)$, the free energy of the activated complex,[40] $\Delta G^{\#} = (\Delta G_{SLRR} + \lambda)^2/4\lambda$ and ΔE_{SLRR}, Eq. 4.[1] After recalling

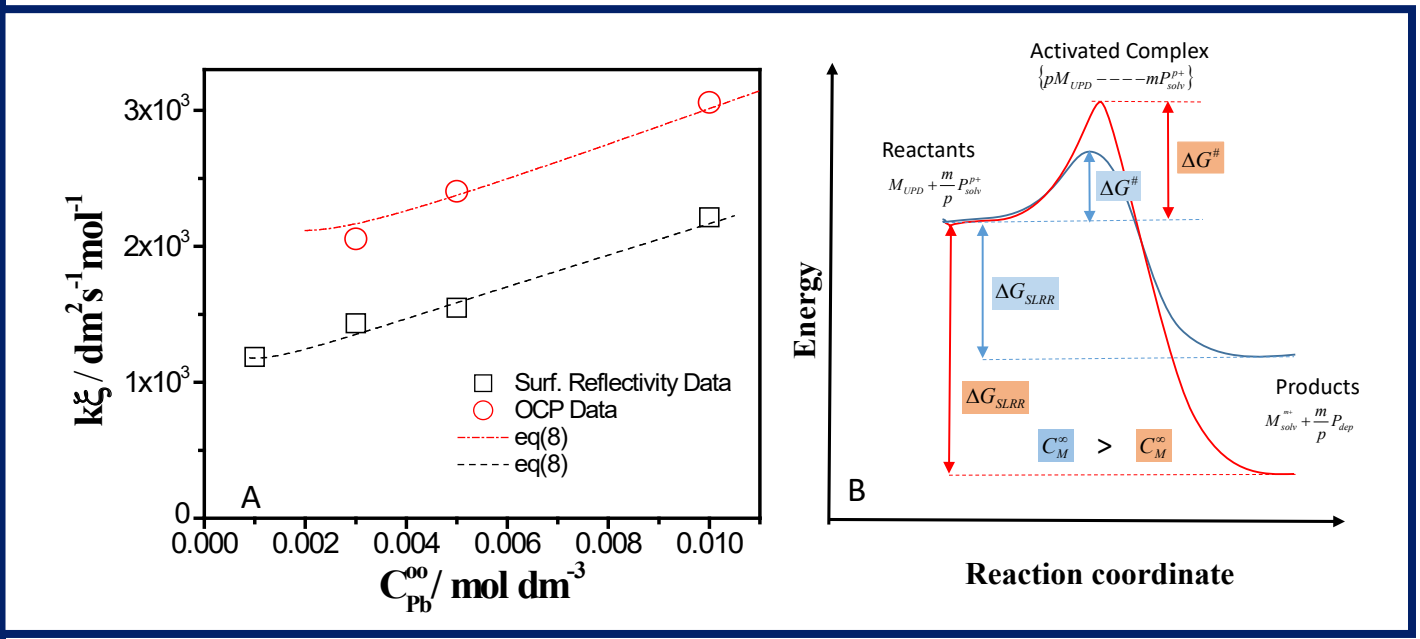

FIG. 4. *(A) Experimental data for the product of fundamental rate constant and interface width (kξ) as a function of Pb^{2+} concentration, C_{Pb}^{∞}, for SLRR reaction: $Pb_{UPD}^{0} + \left(\frac{2}{3}\right) Au_{solv}^{3+} \Rightarrow Pb_{solv}^{2+} + \left(\frac{2}{3}\right) Au_{s}^{0}$; surface reflectivity (black squares); OCP measurements (red circles); and dotted lines represent fits of Eq. 8. (B) Schematics illustrating change of ΔG_{SLRR} and $\Delta G^{\#}$ with increasing C_M^{∞}. Adopted from Ref. 34 with permission.*

the basic thermodynamic relation $\Delta G_{SLRR} = -\frac{m}{p} F \Delta E_{SLRR}$, and assuming that $a_{M^{m+}} \approx C_M^{\infty}$ and $a_{P^{p+}} \approx C_P^{\infty}$, one can show easily that the functional relation between k and C_M^{∞} is given by:

$$k \sim \exp\left(-\frac{\left(\frac{m}{p} F \cdot \left(\Delta E_{\theta\to 0}^{0} - \Delta E_{EMF}^{0} \right) - RT \ln \frac{\left[C_P^{\infty} \right]}{\left[C_M^{\infty} \right]} + \lambda \right)^2}{4\lambda \cdot RT} \right) \quad (8)$$

Here, λ represents the reorganization energy in J.mol^{-1} units while F and R are the Faraday and universal gas constants respectively. The fit of the functional defined by Eq. 8 to kξ versus C_{Pb}^{∞} data is plotted in Fig. 4A, dashed lines. We conclude that increasing the UPD metal ion concentration lowers the free energy for the SLRR reaction, which in turn leads to a lower free energy of the activated complex (energy barrier for SLRR reaction), and this leads to a larger value of the fundamental rate constant. A pictorial form of this conclusion is shown in Fig. 4B.

Additionally, Eq. 8 provides functional describing of the of C_P^{∞} effect on k. Significantly, an increase in C_P^{∞} leads to lower values of k, i.e., C_P^{∞} has an opposite effect on k than C_M^{∞}. However, per Eq. 6 and Eq. 7, the term $\left(C_P^{\infty}\right)^{\zeta}$ is multiplicand in the mathematical description of K_{SLRR}. These apparently conflicting effects of C_P^{∞} on the overall value of K_{SLRR} suggest a complex K_{SLRR} versus C_P^{∞} dependence. Yet, the experimental studies of SLRR kinetics during Au deposition via SLRR of UPD Pb ML show that K_{SLRR} is increasing monotonically with increasing values of C_P^{∞}.[34] Therefore, more experiments with diverse conditions are necessary for a better understanding of the C_P^{∞} effects on K_{SLRR}. As a conclusion, we should emphasize the fact that proper design of the metal ion concentrations in the reaction solution represents an extra "knob" to manipulate the nucleation density and to fine-tune the overall morphology of the deposit obtained by SLRR of UPD ML.

Recent studies that certainly deserve more experimental and theoretical attention demonstrate a large effect of the supporting electrolyte on the fundamental rate constant. Experimental data are shown in Fig. 5 for the SLRR reaction between Au^{3+} and Pb UPD ML on Au(111).[34] The results are intriguing since there is no obvious effect of the supporting electrolyte on reacting species neither is an obvious relation between the supporting electrolyte concentration and the definition of K_{SLRR} or k. Nevertheless, the k versus $C_{HClO_4}^{\infty}$ trend in Fig. 5 can be discussed by considering a basic postulate of the Debye-Huckel theory of electrolyte.[41] A higher $C_{HClO_4}^{\infty}$ in the solution influences the Debye length, λ_D, which is a distance at which the ion charge and Coulomb potential are completely screened by the surrounding ions in solution. For a symmetric supporting electrolyte such as $HClO_4$, the Debye length has $\lambda_D \sim \left(C_{HClO_4}^{\infty}\right)^{-0.5}$ dependence.

Therefore, more perchlorate ions in solution will reduce the value of the Debye length. This means that the effective Coulomb field surrounding a potentially reacting Au^{3+} ion near the surface is felt at shorter distance if the reaction solution contains more $HClO_4$. Because of that, the distance between Au^{3+} and Pb UPD adatoms necessary for effective electron transfer/tunneling has to be shorter. This leads to lower spatial probability of reactive encounter between Pb UPD adatoms and Au^{3+} ions and one could expect slower kinetics of the red-ox process and lower values of the rate constant in solution with higher $C_{HClO_4}^{\infty}$. Therefore, the proper design of the supporting electrolyte concentration in the reaction solution is an elegant way to control the SLRR reaction kinetics and nucleation density and thus to control the morphology of the deposit.

Conclusion and Future Prospects

Future prospects for metal deposition via SLRR of UPD ML are quite exciting. New ideas and approaches focusing on development of diverse protocols with even more possibilities for deposit morphology control are being researched. Along these efforts, one concept that certainly deserves more attention is metal deposition via SLRR of a

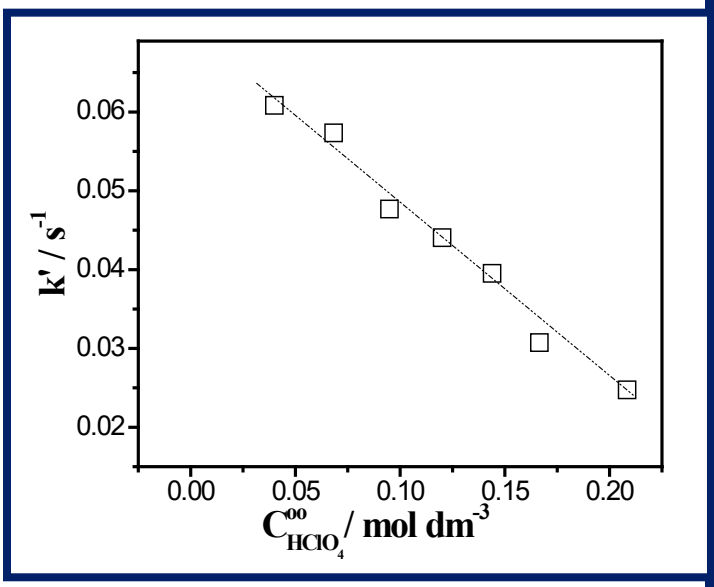

Fig. 5. *Rate constant values plotted as a function of supporting electrolyte concentration. Data obtained from surface reflectivity measurements. Adopted from Ref. 34 with permission.*

UPD ML guided by organic templates.[42] This concept is based on the spatial control of the nucleation probability using an organic phase which shows ordering on the electrode surface in the potential range of the SLRR reaction. The proof of this concept is shown in Fig. 6. The STM image of an organized layer consisting of PTCDI + melamine molecules[43] adsorbed on top of Cu_{UPD}/Au(111) and serving as a template is shown in Fig. 6A. The tri-fold symmetry and organization of the 2D organic phase is evident. The center to center spacing of the unit cells (cages) in the structures is approximately 0.9 nm while the diameter of the empty space within the cell is ~0.7 nm. After SLRR of Cu UPD ML by $\{PtCl_6\}^{2-}$ through the PTCDI + melamine layer, Pt is deposited on Au(111) forming islands/patches consisting of a well-organized population of Pt nanoclusters, Fig. 6B and 6C.[44] The effect of the organic template is obvious, Fig. 6B. The size and organization of Pt nanoclusters replicate the arrangement and symmetry of the organic template, Fig. 6C.

The discussions presented in this article highlight the current understanding of the fundamental relations governing the nucleation process during metal deposition via SLRR of UPD ML. They describe phenomenological links between the reaction solution design, choice of the UPD metal ML and SLRR reaction stoichiometry on the one hand and the SLRR reaction kinetics parameters, nucleation density,[11,16] and resulting morphology of the deposit[4,10] on the other. The general trend is that experimental conditions and solution design leading to SLRR reactions with faster kinetics yield higher nucleation density and deposits with smaller clusters for a given starting coverage of UPD ML. The experimental conditions promoting a larger m/p ratio and lower reaction order in terms of the $\theta_{o,M}$ do promote higher nucleation density and formation of deposits with smaller nanoclusters. These considerations are particularly important when one considers deposition via SLRR of UPD ML for catalyst ML synthesis application.

Design of the optimum experimental conditions for a desired catalyst ML morphology is a function of its application and intended use in a particular reaction. In the case where high activity of the catalyst ML is desired, the conditions promoting low nucleation density and formation of deposit ML morphology with larger nanocluster should be used. However, if poisoning of the catalyst by intermediates hinders the particular reaction kinetics, the synthesis of catalyst ML with modest activity might be beneficial to retain a good reaction yield and the desired reaction pathway.[37] In this case, the conditions promoting high nucleation density and small average size of nanoclusters should be chosen. The same is true if one pursues the

(continued on next page)

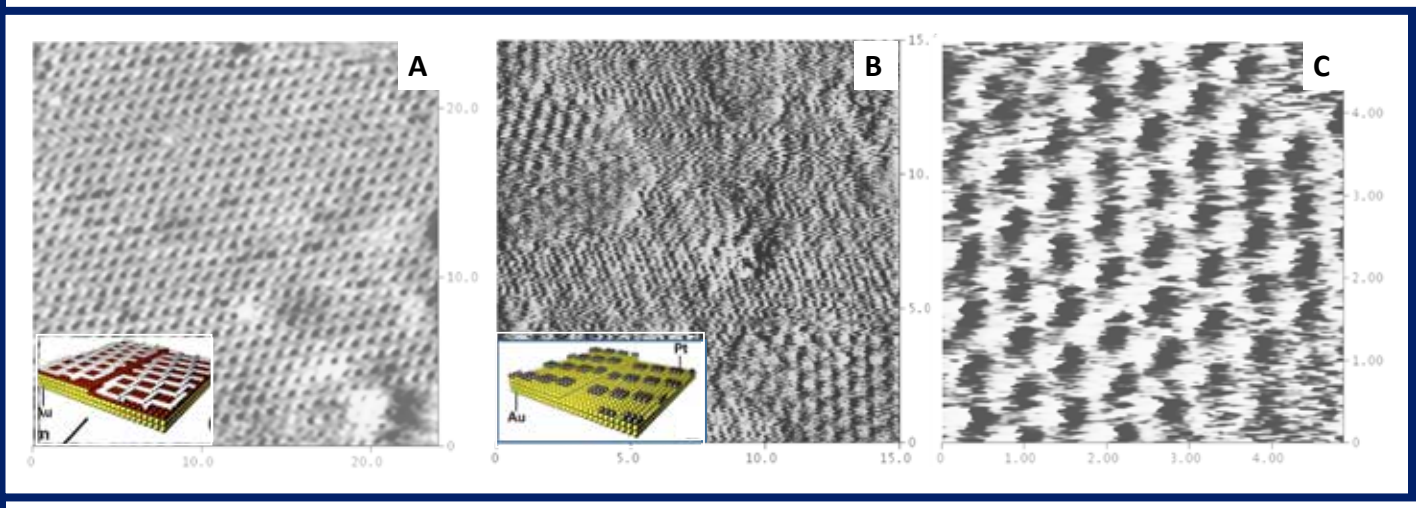

Figure 6. *STM images of: (A) PTCDI + Melamine layer adsorbed on Cu_{UPD}/Au(111), E = −0.V versus SCE in 0.1 M $HClO_4$, image size: 25 × 25* nm. *(B) Pt on Au(111) after SLRR of Cu UPD ML by Pt^{4+} through PTCDI + Melamine layer, image size: 15 × 15 nm. (C) Same as in B, image size 5 × 5 nm. Cartoons of the structures (bottom left) corresponding to the situation in image A and B.*

goal of depositing a high quality homo- and hetero-epitaxial thin films. In conclusion, the considerations presented in this article should be of broader significance for the catalysis and thin film communities as an effort in bridging the gap between the desired properties of metal deposit obtained by SLRR of UPD ML and the required conditions for its synthesis.

Acknowledgment

The author greatly acknowledges financial support from the National Science Foundation under the grants CHE-0955922 and CBET 1605331.

About the Author

Stanko R. Brankovic is a professor in the Department of Electrical and Computer Engineering and the Department of Chemical and Biomolecular Engineering at the University of Houston. His research is focused towards better understanding of the physical and chemical processes at the electrochemical interface and their use in producing materials and nanostructures with novel functionality and applications. The diverse and multidisciplinary nature of his research spans the areas of sensors, magnetic materials, thin films, electrocatalysis, and nanofabrication. He may be reached at SRBrankovic@uh.edu.

References

1. S. R. Brankovic, J. X. Wang, and R. R. Adzic, *Surf. Sci.*, **474,** L173 (2001).
2. K. Sasaki, J. X. Wang, H. Naohara, N. Marinkovic, K. More, H. Inada, and R. R. Adžić, *Electrochim. Acta,* **55**, 2645 (2010).
3. A. Nilekar, Y. Xu, J. Zhang, M. Vukmirovic, K. Sasaki, R. Adžić, and M. Mavrikakis, *Top. Catal.,* **46,** 276 (2007).
4. N. Dimitrov, *Electrochim. Acta*, **209**, 599 (2016).
5. M. B. Vukmirovic, S. T. Bliznakov, K. Sasaki, J. X. Wang, and R. R. Adzic, *Electrochem. Soc. Interface*, **20**, 33 (2011).
6. Y. G. Kim, J. Y. Kim, D. Vairavapandian, and J. L. Stickney, *J. Phys. Chem. B*, **110,** 17998 (2006).
7. C. Mitchell, M. Fayette, and N. Dimitrov, *Electrochim. Acta,* **85**, 450 (2012).
8. J. Nutariya, M. Fayette, N. Dimitrov, and N. Vasiljevic, *Electrochim. Acta*, **112**, 813 (2013).
9. S. R. Brankovic, N. Vasiljevic, N. Dimitrov in *Modern Electroplating V*, M. Paunovic and M. Schlesinger, Editors, p. 573, John Willey and Sons, Inc. New York, NY (2010).
10. S.-E. Bae, D. Gokcen, P. Liu, P. Mohammadi, and S. R. Brankovic, *Electrocatalysis*, **3**, 203 (2012).
11. D. Gokcen, Q. Yuan, and S. R. Brankovic, *J. Electrochem. Soc.*, **161**, D3051 (2014).
12. M. Fayette, Y. Liu, D. Bertrand, J. Nutariya, N. Vasiljevic, and N. Dimitrov, *Langmuir*, **27**, 5650 (2011).
13. L. T. Viyannalage, R. Vasilic, and N. Dimitrov, *J. Phys. Chem. C*, **111**, 4036 (2007).
14. J. Zhang, K. Sasaki, E. Sutter, and R. R. Adžić, *Science* **315**, 220 (2007).
15. R. Loukrakpam, Q. Yuan, V. Petkov, L. Gan, S. Rudi, R. Yang, Y. Huang, S. R. Brankovic, and P. Strasser, *Phys. Chem. Chem. Phys.*, **16**, 18866 (2014).
16. D. Gokcen, S.-E. Bae, and S. R. Brankovic, *J. Electrochem. Soc.*, **157,** D582 (2010).
17. D. Gokcen, S.-E. Bae, and S. R. Brankovic, *Electrochim. Acta*, **56**, 5545 (2011).
18. S. Trasatti, *J. Electroanal. Chem.,* **33**, 351(1971); and references therein.
19. D. M. Kolb in *Advances in Electrochemical Eng.*, H. Gerischer and W. Tobias, Editors, Wiley & Sons, New York (1978); and references therein.
20. E. Budevski, G. Staikov, and W. J. Lorenz in *Electrochemical Phase Formation and Growth*, R. C. Alkire, P. N. Bartlett, and J. Lipkowski, Editors, p. 41, VCH, Berlin (1996); and references. therein.
21. E. Herrero, L. J. Buller, and H. D. Abruña, *Chem. Rev.*, **101**, 1897 (2001).
22. M. Will, M. Dietterle, and D. Kolb, in *Nanoscale Probes of the Solid/ Liquid Interface*, Vol. 288, A. Gewirth and H. Siegenthaler, Editors, p 137-162, Springer, Berlin (1995).
23. S. Garcia, D. Salinas, and G. Staikov, *Surf. Sci.*, **576**, 9 (2005).
24. S. Corcoran, G. Chakarova, and K. Sieradzki, *J. Electranal. Chem.,* **377**, 85 (1994).
25. M. Esplandiu, M. Schneeweiss, and D. Kolb, *Phys. Chem. Chem. Phys.,* **1**, 4847 (1999).
26. K. Engelsmann, W. Lorenz, and E. Schmidt, *J. Electroanal. Chem.,* **114**, 1 (1980).
27. E. Schmidt, H. Gygax, and P. Bohlen, *Helv. Chim. Acta,* **49**, 733 (1966).

28. R. Adzic, E. Yeager, and B. Cahan, *J. Electrochem. Soc.,* **121**, 474 (1974).
29. A. Bewick and B. Tomas, *J. Electroanal. Chem.,* **84**, 127 (1977).
30. S. Swathirajan and S. Bruckenstein, *Electrochim. Acta,* **28**, 865 (1983).
31. I. V. Markov, *Crystal Growth for Beginners*, World Scientific, NY (1995).
32. S. Stoyanov and D. Kashchiev, in *Current Topics in Material Acience*, Vol. **7**, E. Kaldis, Editor, p. 69, North Holland, NY (1981).
33. J. A. Venables, G. D. Spiller, and M. Hanbucken, *Rep. Prog. Phys*., **47**, 339 (1984).
34. E. Bulut, D. Wu, N. Dole, H. Kilic, and S. R. Brankovic, *J. Electrochem. Soc.,* **164**, D159 (2017).
35. J. M. Smith, *Chemical Engineering Kinetics*, 2nd edition, p. 47 and 52, McGraw Hill, New York (1970).
36. S. R. Brankovic and G. Zangari in *Electrochemical Engineering Across Scales: From Molecules to Processes*, R. C. Alkire, P. N. Bartlett, and J. Lipkowski, Editors, p. 59-107, Wiley-VCH, New York (2015).
37. Q. Yuan, H. A. Doan, L. Grabow, and S. R. Brankovic, *J. Am. Chem. Soc.,* **139**, 13676 (2017).
38. K. Sieradzki, S. R. Brankovic, and N. Dimitrov, *Science*, **284**,138 (1999).
39. S. Glasstone, K. J. Laidler, and H. Eyring, *The Theory of Rate Processes,* McGraw-Hill, New York (1941).
40. R. A. Marcus, *Annu. Rev. Phys. Chem.* **15**, 155 (1964).
41. P. Debye and E. Hückel, *Phyz Z.* **24,** 185 (1923).
42. D. Gokcen, O. Miljanic, and S. R. Brankovic, Abstract 2051, *The Electrochemical Society Meeting Abstracts,* MA 2010-02, Las Vegas, NV, Oct. 10-15 (2010).
43. R. Madueno, M. T. Raeisaenen, C. Silien and M. Buck, *Nature*, **454**, 618 (2008)
44. D. Gokcen, O. Š. Miljanić, and S. R. Brankovic, Abstract 2443, *The Electrochemical Society Meeting, Abstracts,* MA 2009-02, Vienna, Austria, Oct. 4–9 (2009).